REPORT DOCUMENTATION PAGE

AFRL-SR-AR-TR-05-

0418

1. REPORT DATE (DD-MM-YYYY)	2. REPORT TYPE	3. DATES COVERED (From - To)
31-8-2005	Final	April 1-2002-Aug. 31, 2005

4. TITLE AND SUBTITLE
Ultrawideband Radio Frequency (RF) Enhanced Electroporation for Chemotherapy

5a. CONTRACT NUMBER

5b. GRANT NUMBER
F49620-02-1-0174

5c. PROGRAM ELEMENT NUMBER

6. AUTHOR(S)
R.M. Gilgenbach, Y.Y. Lau, M.D. Uhler and D. Jordan

5d. PROJECT NUMBER

5e. TASK NUMBER

5f. WORK UNIT NUMBER

7. PERFORMING ORGANIZATION NAME(S) AND ADDRESS(ES)
University of Michigan
Ann Arbor, MI 48109

NE

8. PERFORMING ORGANIZATION REPORT NUMBER

9. SPONSORING/MONITORING AGENCY NAME(S) AND ADDRESS(ES)
Air Force Office of Scientific Research
4015 Wilson Blvd.
Arlington, VA 22203

10. SPONSOR/MONITOR'S ACRONYM(S)
AFOSR

11. SPONSOR/MONITOR'S REPORT NUMBER(S)

12. DISTRIBUTION/AVAILABILITY STATEMENT
Unlimited

DISTRIBUTION STATEMENT A
Approved for Public Release
Distribution Unlimited

13. SUPPLEMENTARY NOTES
none

14. ABSTRACT
Experimental results are presented for a research program in which high voltage, short-pulsed, ultrawideband electric fields have been demonstrated to enhance the effects of chemotherapy upon killing of Jurkat (cancer) cells. Electric fields of about 100 kV/cm have been shown to enhance the killing of Jurkat cells by up to a factor of 1,000 over a low dose of the drug bleomycin. Enhancement of chemotherapy was also found at lower electric fields of 50 kV/cm and higher electric fields up to 200 kV/cm. The cellular mechanism by which the electric fields enhance cell death occurs appears to be independent of caspase activation and hence does not involve classical apoptosis. Rather, the lack of caspase involvement in the UWB mediated cell killing is consistent with "pseuodapoptosis" observed previously with high concentrations of bleomycin. Earlier experiments explored the effects of narrowband RF on conventional electroporation. Addition of radio frequency modulation to a standard electroporation pulse (without drugs) was found to increase the overall yield of live, electroporated cells by improving the survivability.

15. SUBJECT TERMS
ultrawideband radiation, electroporation, chemotherapy

16. SECURITY CLASSIFICATION OF:			17. LIMITATION OF ABSTRACT	18. NUMBER OF PAGES	19a. NAME OF RESPONSIBLE PERSON
a. REPORT	b. ABSTRACT	c. THIS PAGE			Ronald M. Gilgenbach
U	U	U	UU	31	19b. TELEPHONE NUMBER (Include area code) 734-763-1261

FINAL TECHNICAL REPORT TO:

Dr. ROBERT J. BARKER
THE AIR FORCE OFFICE OF SCIENTIFIC RESEARCH

FOR THE PROJECT:
Ultrawideband Radio Frequency (RF) Enhanced Electroporation for Chemotherapy

AFOSR GRANT NUMBER: F49620-02-1-0174

SUBMITTED BY:

RONALD M. GILGENBACH, PROFESSOR
Y.Y. LAU, PROFESSOR,
MICHAEL D. UHLER PROFESSOR and
DAVID JORDAN, GRADUATE STUDENT
UNIVERSITY OF MICHIGAN
ANN ARBOR, MI 48109-2104

August 2005

AFOSR Grants Officer: Jennifer L. Bell

Ultrawideband Radio Frequency (RF) Enhanced Electroporation for Chemotherapy
AFOSR GRANT NUMBER: F49620-02-1-0174

TABLE OF CONTENTS

Page

1.0 EXECUTIVE SUMMARY..... 3

2.0 Experimental Configuration..... 4

3.0 Summary of Experimental Results..... 6

4.0 Theory..... 25

5.0 Student, Faculty and Staff Involvement in This Research..... 28

6.0 Relevant Publications and Conference Papers by UM Faculty and Students..... 29

1.0 EXECUTIVE SUMMARY

Experimental results are presented for a research program in which high voltage, short-pulsed, ultrawideband electric fields have been demonstrated to enhance the effects of chemotherapy upon killing of Jurkat (cancer) cells. Electric fields of about 100 kV/cm have been shown to enhance the killing of Jurkat cells by up to a factor of 1,000 over a low dose of the drug bleomycin. Enhancement of chemotherapy was also found at lower electric fields of 50 kV/cm and higher electric fields up to 200 kV/cm. The cellular mechanism by which the electric fields enhance cell death occurs appears to be independent of caspase activation and hence does not involve classical apoptosis. Rather, the lack of caspase involvement in the UWB mediated cell killing is consistent with "pseuodapoptosis" observed previously with high concentrations of bleomycin.

Earlier experiments explored the effects of narrowband RF on conventional electroporation. Addition of radio frequency modulation to a standard electroporation pulse was found to increase the overall yield of live, electroporated cells by improving the survivability; those experiments were performed with dye rather than electroporation drugs.

2.0 **Experimental Configuration for Ultrawideband Cell Exposure**

(from David Jordan Doctoral Dissertation)

A termination device for the UWB pulser was subject to several rigorous performance requirements. To achieve optimum risetime and pulse voltage performance, the UWB pulser required a 50 Ohm broadband matched load. To provide an acceptable RF exposure system for bioeffects experiments, the device was required to produce predictable and reproducible electric field distributions at the location of the biological samples. The device was also required to withstand the high voltage applied by the UWB pulser without arcing. Finally, a high degree of RF shielding was desired to isolate the experiment's radiated RF/EMP emissions from personnel, experimental diagnostics, and other electronic equipment.

A custom broadband high voltage load was devised, based on a tapered transmission line. The device, depicted in Fig. 2.1, was a two-conductor planar transmission line, constructed from two roughly triangular sheets of copper. Both the electrode spacing and width of the conductors increased from input to termination, providing varying electric field strengths along the length of the device while maintaining 50 Ohm characteristic impedance. The line was terminated by a parallel quartet of 200-Ohm, Carborundum, low-inductance, high-power resistors to provide a 50 Ohm electrical termination, Fig. 2.1. The entire assembly was housed in a wooden enclosure. The walls of the enclosure were lined with copper sheeting for shielding and microwave absorber to attenuate radiated emissions. The load was connected to the UWB pulser by 10 meters of RG-217 high-voltage coaxial cable.

When the initial enclosure was discovered to have a strong cavity resonance at 2 GHz, creating large UWB signal reflections, a larger enclosure was designed with at least 20 cm clearance between the UWB load and the walls on all sides. The final assembly comprised a nonresonant cavity structure, permitting broadband operation.

Near the input port of the planar transmission line, a pair of copper strips were attached to the electrodes and connected to a cuvette holder. This was done to provide a method for direct UWB exposure of cells in cuvettes and to achieve higher electric fields than those available between the planes of the transmission line. Although not strictly a GTEM cell, the final assembly was designated GTEM-IIIC. Figure 2.1 illustrates top and side views of the GTEM-IIIC with the cuvette holder and termination resistors installed.

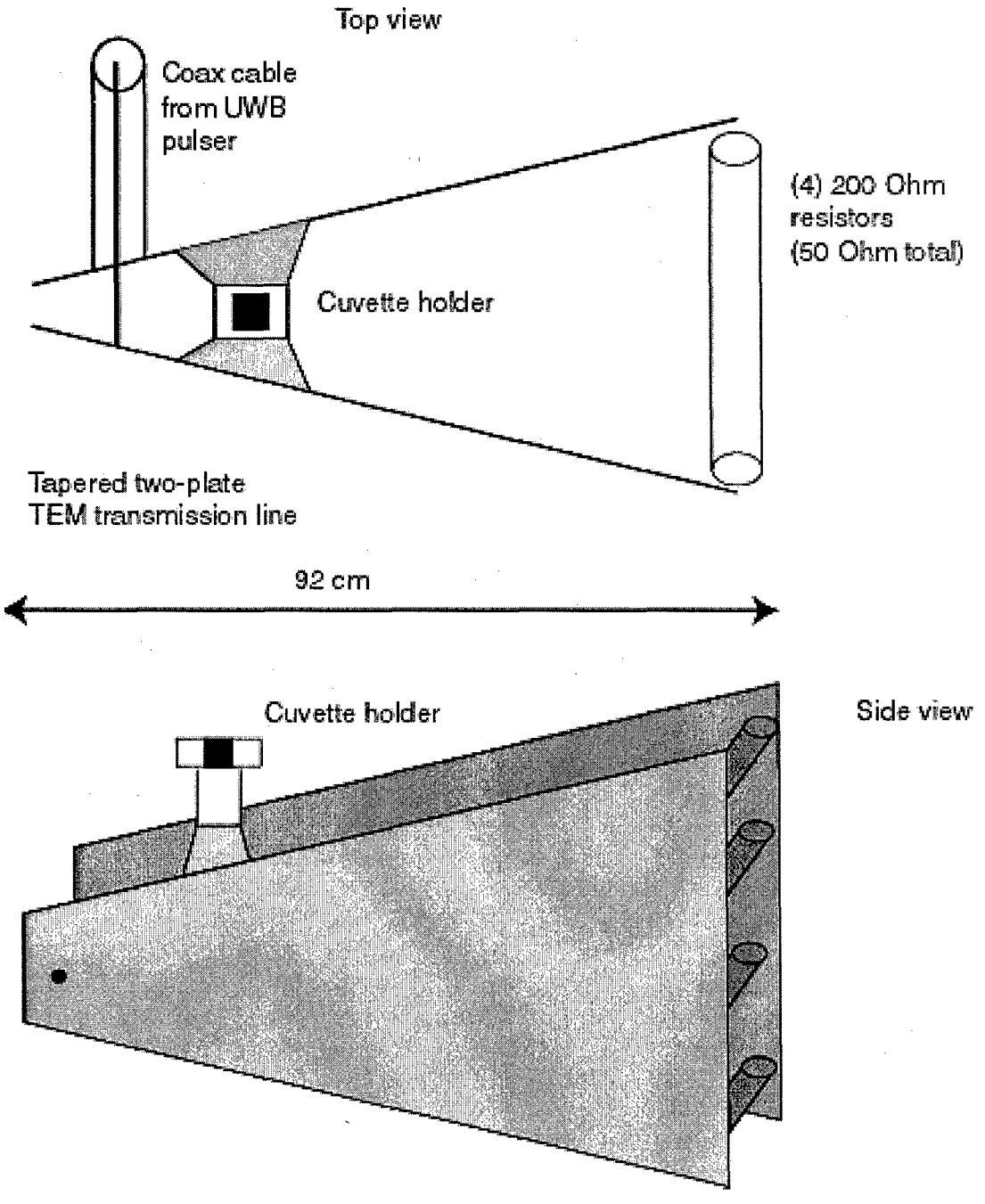

Figure 2.1. GTEM-IIIC UWB load and exposure system with cuvette holder and resistors installed. Note that cuvette holder and cable (shown in top view) are not to scale.

3.0 Summary of Experimental Results

ENHANCEMENT OF CANCER CHEMOTHERAPY IN VITRO BY INTENSE ULTRAWIDEBAND ELECTRIC FIELD PULSES (from UM Doctoral Dissertation of David Jordan)

As an extension of work focusing on the use of conventional electroporation (EP) to deliver chemotherapeutic agents such as bleomycin to tumor cells, experiments were performed to determine the effectiveness of very short (sub-microsecond) pulses at very high (~ 100 kV/cm) electric fields in electroporative delivery of such agents. A characterization of the pulses delivered by the Titan peaking circuit generator was performed. Possible thermal effects of the UWB pulse treatments were also investigated and ruled out as a significant contribution. Cellular response to various combinations of electric field treatment and drug treatment was determined in terms of cell viability and possible mechanisms of cell death. In particular, markers of apoptosis were measured at several time points to determine the evolution of the cell population following exposure to ultrawideband (UWB) pulses and bleomycin, or ultrawideband electrochemotherapy (UWB ECT).

3.1 UWB Pulse Diagnostics

Pulse exposures of cell samples were performed with a typical UWB pulse applied to a cell sample at a peak voltage of approximately -20 ± 3 kV, resulting in peak electric fields of approximately 50, 100, or 200 kV/cm across a 4 mm, 2 mm, or 1 mm electrode gap, respectively. BTX electroporation cuvettes were used in all exposures. A typical UWB pulse waveform is presented in Figure 3.1; the pulser was charged to -40 kV. This pulse was measured across a 4 mm cuvette electrode gap loaded with HBSS buffer. The voltage reported was measured on the initial voltage spike resulting from the fast discharge of the peaking capacitor. The "tail" discharge typically lasted about 200 ns with an average voltage of -9 ± 1 kV, followed by a voltage reversal of 6.5 ± 1.5 kV (with positive polarity) lasting an additional 200 ns. Slight variation was observed in the peak voltages for different cuvette sizes due to different impedances and matching conditions. For each sample, the maximum peak voltages for all pulses in the applied pulse train were averaged to produce an "average peak voltage" for the sample. This value was recorded for each experiment. All waveforms were captured using a 6 GHz, 20 GS/s digital sampling oscilloscope and stored in a PC by LabVIEW.

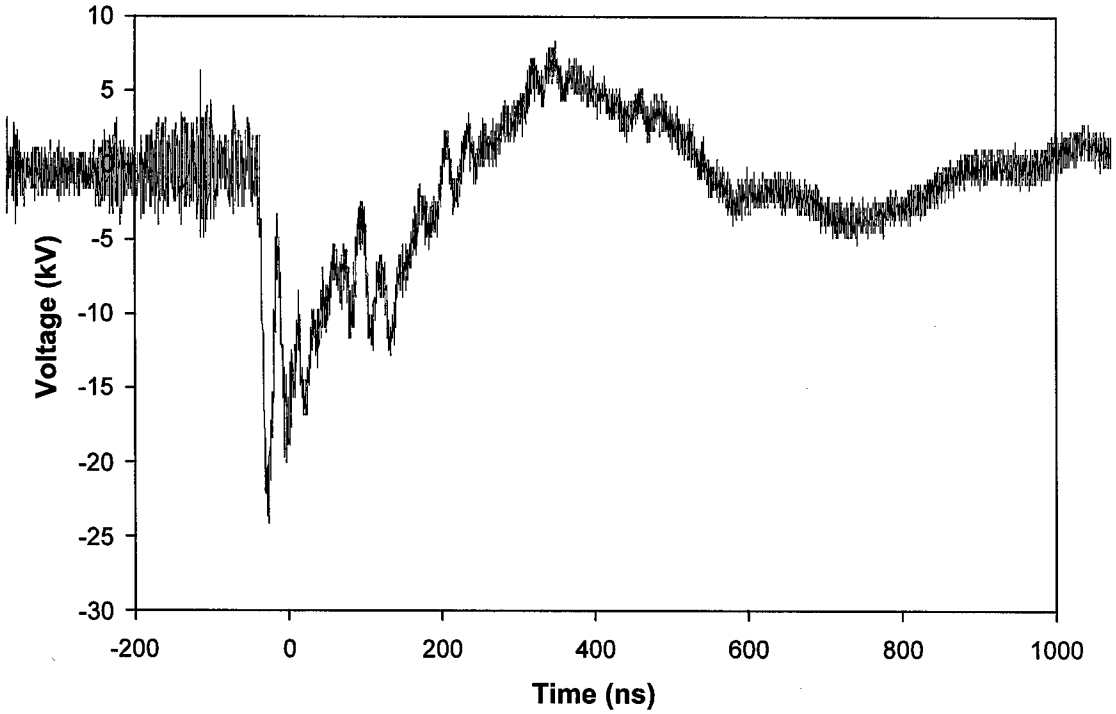

Figure 3.1. Typical UWB output pulse measured across biological load.

While the recorded waveforms were considered representative of the exposure conditions for the cell samples, the frequency content of the pulses could not be adequately determined. The high voltage probe used in these experiments was band-limited with a factory-installed 150 MHz low-pass filter due to a physical probe resonance at 200 MHz. The UWB generator was designed to produce sub-nanosecond risetime and was factory tested to achieve a 920 ps risetime into a matched load (requiring > GHz measurement bandwidth). Accordingly, it was assumed that the recorded waveforms, while giving a good representation of the temporal behavior of the pulse, lacked sufficient temporal resolution to adequately measure the pulse's true frequency content.

A time-frequency analysis of an early test pulse confirmed this behavior. The test waveform and time-frequency analysis plot are depicted in Figure 3.2. The signal intensity at each time and frequency is represented by the color shading, with red representing the highest spectral power density, yellow representing intermediate power, and blue representing the lowest power. The absence of any signal content above 100 MHz confirmed the expectation that the internal band-limiting of the probe either cut off higher-frequency components or measured fast-rising signals with slower risetime, or both.

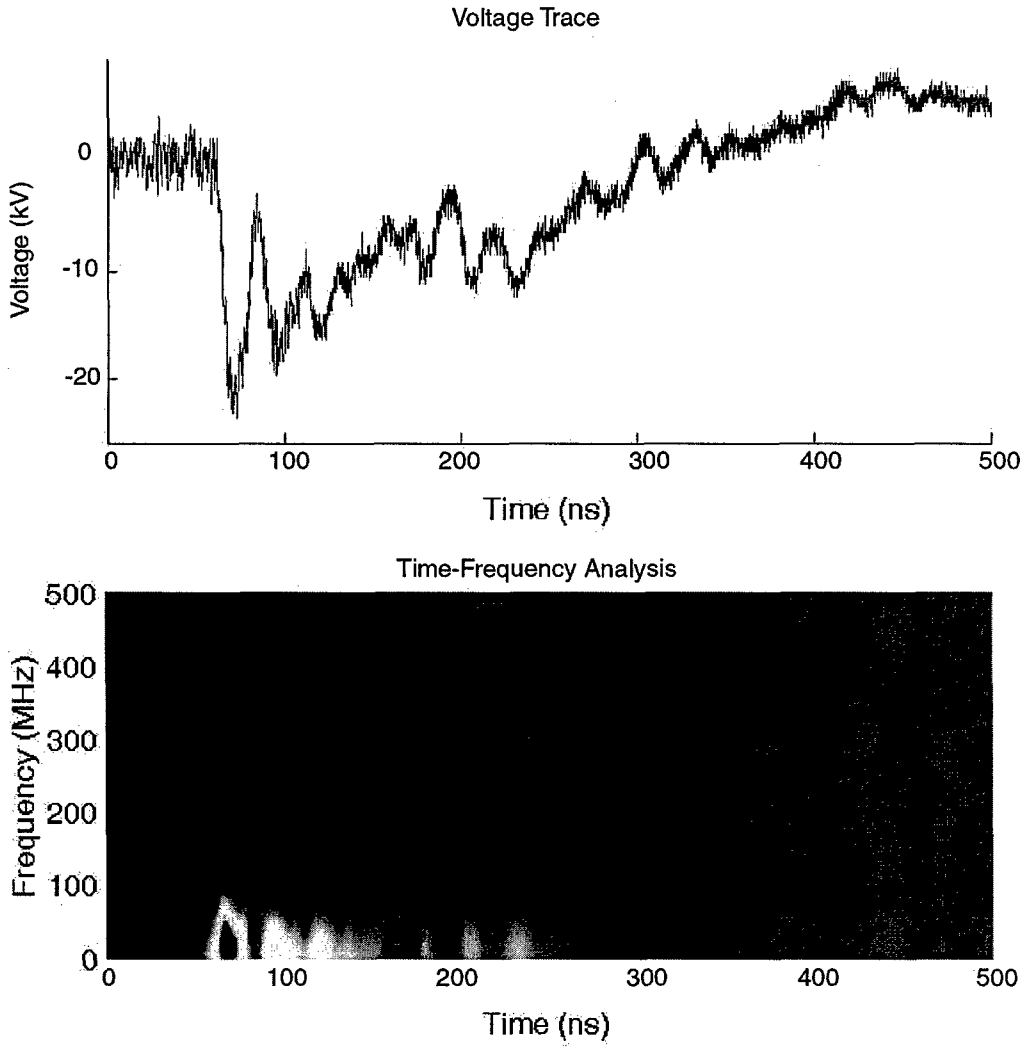

Figure 3.2. Time-frequency analysis of UWB test pulse.

The current through the cuvette was measured directly using a Pearson 110A current monitor on several test shots. The average current through a 2-mm gap filled with HBSS was -2.24 ± 0.04 kA for a -40 kV charge which produced -18 kV peak voltage across the load. This measurement was consistent with the low-voltage long-pulse I-V characteristics for the cuvettes, and direct measurement of current was discontinued for subsequent experiments due to the difficulty of insulating the current probe and measurement circuit from high voltage in the experiment.

Sample Heating and Thermal Effects

Given the high (~MW) peak powers deposited in the biological samples and the sensitivity of biological systems to temperature, thermal effects were investigated as a potential source of biological response in UWB exposure experiments. Cuvettes loaded with HBSS or suspensions of Jurkat cells in HBSS were exposed to UWB for cases

expected to cause maximum Ohmic heating: minimum sample size, maximum electric field, and maximum pulse train length. The temperature of each sample was measured *in situ* at the beginning and end of the pulse exposure with a thermocouple. Resistance was determined separately for the mixtures of buffer solution and culture media by recording I-V curves with 100-μs pulses. The results are summarized in Table 3.1.

Sample	Resistance (Ω)	dT (°C)	# pulses	dT/pulse (°C)
HBSS	13.5	7.5	100	0.075
50% HBSS, 50% RPMI	21.8	2.2	100	0.022
25% HBSS, 75% RPMI	20.2	6.3	100	0.063
RPMI	15.6	5.0	102	0.049
Jurkat cells in HBSS	--	3.8	100	0.038

Table 3.1. Temperature rise in biological samples exposed to long trains of UWB pulses at 200 kV/cm peak field strength.

Sample temperatures were 22-23 °C at the beginning of the pulse trains. The sample volumes were small enough to equilibrate to room temperature rapidly. This was also true of cell suspensions prepared and incubated at 37° C.
Mixtures of RPMI culture medium with HBSS were investigated as a possible substitute for pure HBSS buffer in cell suspensions due to the higher resistivity of the mixtures. These mixtures were tested to better match the cuvette impedance to the 50 Ω output impedance of the UWB pulser. However, the mixtures caused frequent arcing through the cuvette during pulse exposure. Arcing was undesirable due to the generation of free radicals that would have unpredictable effects on cells, so only pure HBSS was used in experiments with cells.

Throughout all conventional electroporation experiments cells in sham-exposed samples tolerated the transition to room temperature and return to a 37° C incubator with negligible effects on cell viability. Consequently, all temperatures in the range of 22 – 37° C were considered a safe range for cells. It was clear from the data in Table 3.1 that under even the most extreme UWB pulse exposure conditions, cell samples were not subjected to sufficient temperatures to generate a hyperthermia or heat shock response. As an additional margin of safety, cells typically would not be expected to exhibit a hyperthermia response below a temperature of approximately 40° C, a temperature threshold which was never approached in these trials. Consequently, thermal biological responses due to Ohmic heating of samples was rejected as a source of biological effects in UWB exposure experiments.

Cytotoxicity of UWB Pulse Exposures

Jurkat cells exposed to trains of UWB pulses at ~ 95 kV/cm were assessed for viability at 24 hours post-exposure using trypan blue staining. The pulse repetition rate was 1 Hz. The results are depicted in Figure 3.3. Data were not normalized since survival of sham-exposed controls was 97%. The data showed a general agreement with the results reported by Pakhomov for Jurkat and U937 cells.

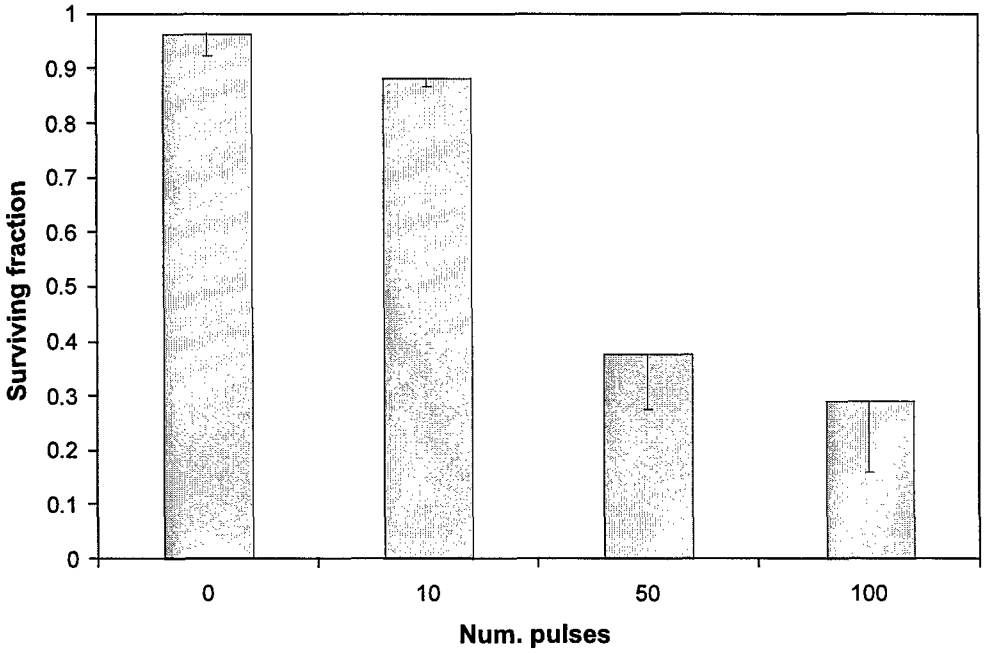

Figure 3.3. Cytotoxicity of 95 kV/cm UWB electric field pulse trains.

A simple exponential fit to these data produced the following relationship to predict cell killing due to 95 kV/cm UWB pulses:

$$S = 0.92e^{-0.0127n} \tag{3-1}$$

where S was the fraction of cells surviving the exposure and n was the number of pulses applied at 1 Hz repetition rate. Thus, on average a train of 48 pulses was expected to produce 50% cell killing.

The mechanism of UWB killing in these experiments was of interest. Despite theoretical and experimental evidence that the primary interaction of UWB electric fields was expected to be with cellular and intracellular membranes, and not with DNA, previous results and preliminary data indicated that cell killing could be characterized using models from radiobiology developed for cell death due to DNA damage. In fact, the classical dose-response curve in radiobiology resembles Figure 3.3, with radiation dose plotted on the x-axis in place of pulse train length. Such curves typically exhibit a transition from a shallow to steep slope at a "knee" or "shoulder." Two dose-response models were borrowed from radiobiology to investigate the role of UWB pulses in cell killing.

The first, the quasi-threshold model, was used in previous published UWB cell-killing studies to fit experimental data. This model, also known as the multitarget model, is considered to be of limited use in radiobiology because it fails to give detailed information about the microscale interaction of ionizing radiation with cellular components, in particular the type of DNA damage caused by X-rays, gamma rays, and particle radiation. However, the quasi-threshold model provides a useful prediction of cell killing extrapolated over a range of radiation doses. For these experiments, the number of applied UWB pulses was considered to be analogous to radiation dose in x-ray experiments.

The model characterizes the shape of the killing curve with two constants, each corresponding to an exponential slope. The initial slope, D_1, is attributed to killing events in which a single radiation interaction caused cell death. The final slope, D_0, describes a killing curve where cell death occurred due to multiple radiation interactions. A third parameter, the quasi-threshold dose D_q, identifies the dose at which the measured killing curve transitions from the slope D_1 to the slope D_0. At doses below the quasi-threshold dose D_q, the survival of cells is given by

$$S = e^{\frac{-D}{D_1}}, \tag{3-2}$$

while the survival for doses above D_q is given by

$$S = e^{\frac{-D}{D_0}}. \tag{3-3}$$

A killing curve for mammalian cells exposed to x-rays is characterized by $D_0 > D_1$. Cell killing data were graphed in Figure 3.4 with two fit lines depicting the dose slopes D_1 and D_0. These slopes did not indicate that the cells had a quasi-threshold type response. The initial and final "doses" were calculated to be 163 and 182 pulses, respectively. Given that these values differed from each other by less than 20%, it is unlikely that the killing mechanism of the UWB pulses warranted the use of such a model of cell killing. Apparently short and long pulse trains killed cells by the same mechanism, and only the magnitude of cell killing varied with pulse train length.

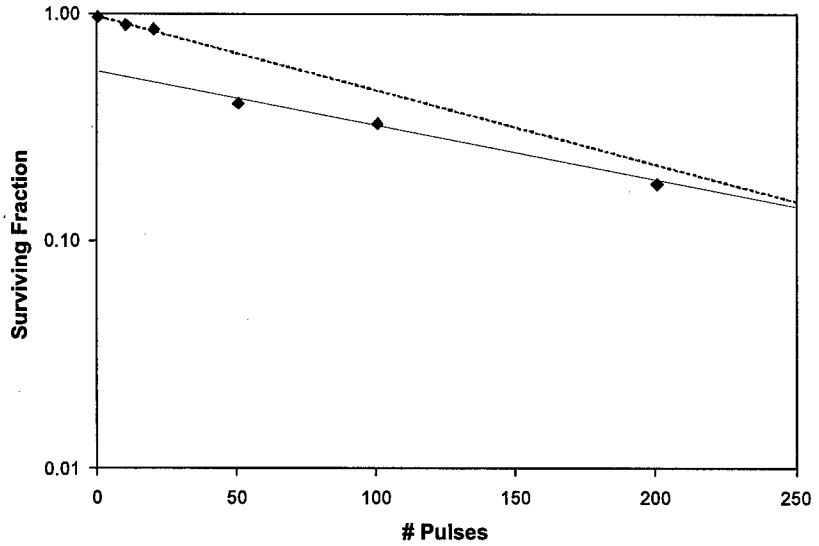

Figure 3.4. UWB cell killing with quasi-threshold model fitted to cell killing data.

The second cytotoxicity model in radiobiology is the linear-quadratic model. This model expresses cell survival as a function of dose, but a single expression is used for survival at all doses:

$$S = e^{-\alpha D - \beta D^2} \tag{3-4}$$

In the linear-quadratic model, the α and β terms denote killing contributions due to different types of chromosome aberrations produced by ionizing radiation. This model has been found to correlate well to microscale observations of such chromosomal aberrations in mammalian cells.

The data from Figure 3.3 were fitted to such a model, with the result that α and β terms of opposite sign were recovered. This result was unphysical and resulted in the conclusion that the mechanisms giving rise to linear-quadratic killing models were not responsible for cell killing in the UWB exposures.

UWB-Enhanced Chemotherapy: Cytotoxicity of UWB-Mediated Bleomycin Delivery

Jurkat cells were suspended in HBSS with an added 5 μM bleomycin concentration and exposed to trains of UWB pulses at 95 kV/cm peak electric field strength. Viability was assessed at 24 hours post-exposure by trypan blue staining. The results of these measurements are compared in Figure 3.5 to the killing values reported in Figure 3.3 for UWB exposures without bleomycin.

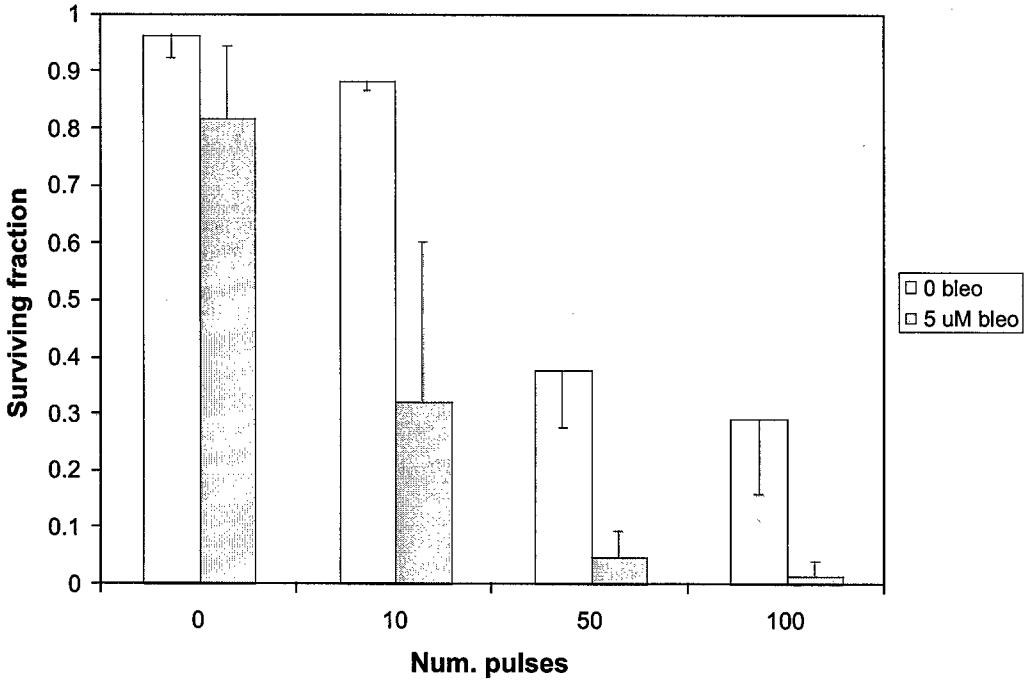

Figure 3.5. Cytotoxicity of bleomycin and 95 kV/cm UWB pulses.

The application of UWB electric field pulses dramatically increased the killing effect of a 5 μM bleomycin dose. Although much longer pulse trains were required to achieve this effect for UWB pulses compared to 100 μs pulses, it was clear that for a pulse train resulting in slightly more than 50% killing, a very high degree of killing could be achieved with the addition of a very low concentration of bleomycin. This result suggested that the UWB pulses permeabilized the cell membranes to allow bleomycin to interact with cellular DNA, consistent with the predictions.

Figure 3.6 illustrates qualitatively the differences between the cell killing results for different combinations of UWB pulse treatments and bleomycin treatments, observed by trypan blue staining. These light micrographs showed that while the bleomycin dose

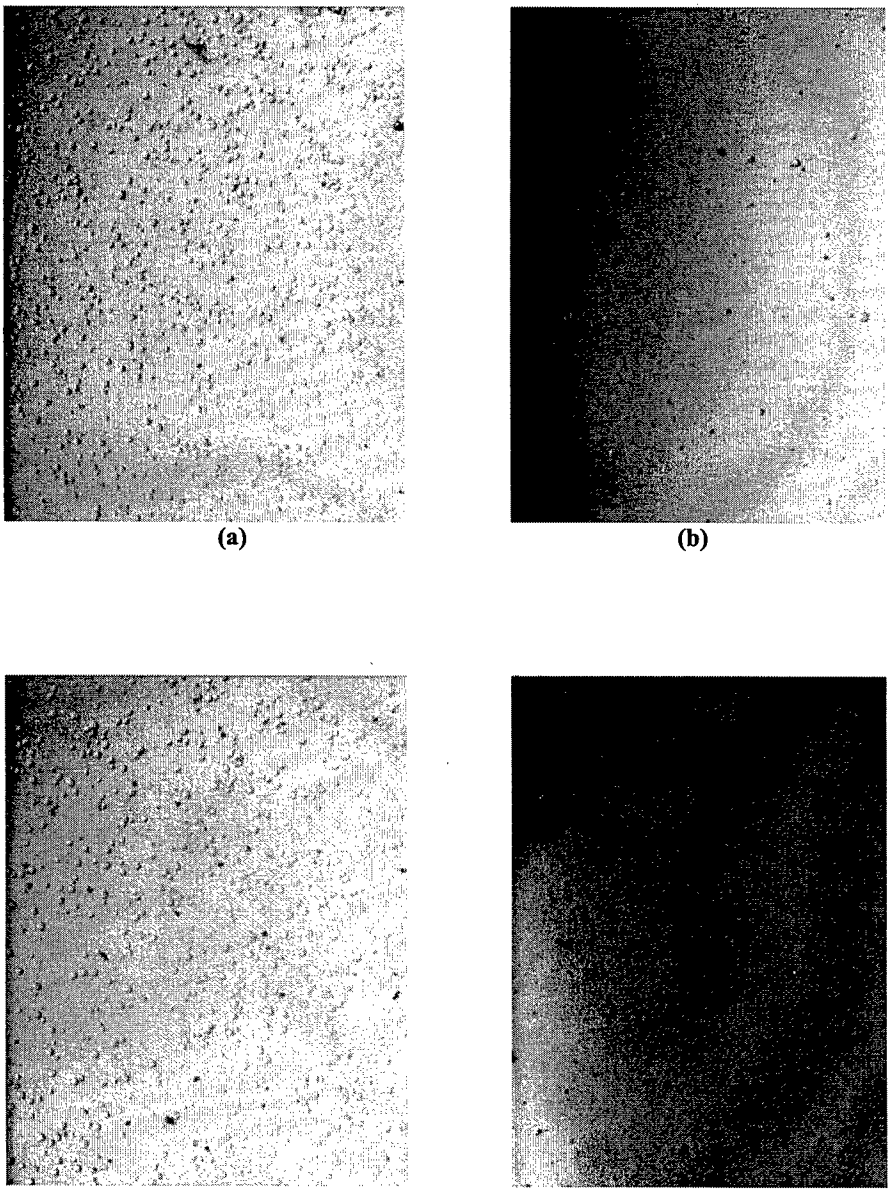

Figure 3.6. Micrographs of trypan blue-stained Jurkat cells 24 hours after UWB pulse and 5 μM bleomycin treatment. Dark cells are dead.
(a) Untreated (sham) control cells.
(b) Cells subjected to 100 pulses in the absence of bleomycin.
(c) Cells subjected to 5 μM bleomycin only (no pulses).
(d) Cells subjected to 100 pulses and 5 μM bleomycin.

increased the proportion of dead (dark-stained) cells in a given sample, the UWB pulse treatment reduced the overall density of the cell population, indicating very fast killing of cells which subsequently disintegrated during the 24 hour incubation period. The similarity of this behavior to the results observed for longer pulses at lower voltage suggested that the most important interaction of the UWB pulses was with the membranes of the cells, as was the case for conventional EP pulses.
This reduction in cell density was quantified by measuring the cell culture densities on a hemocytometer. Only live cells (trypan blue-negative) were counted. The data in Figure 3.7 confirmed that a train of 50 UWB pulses improved the killing effect of a 5 μM bleomycin dose by more than a factor of 100.

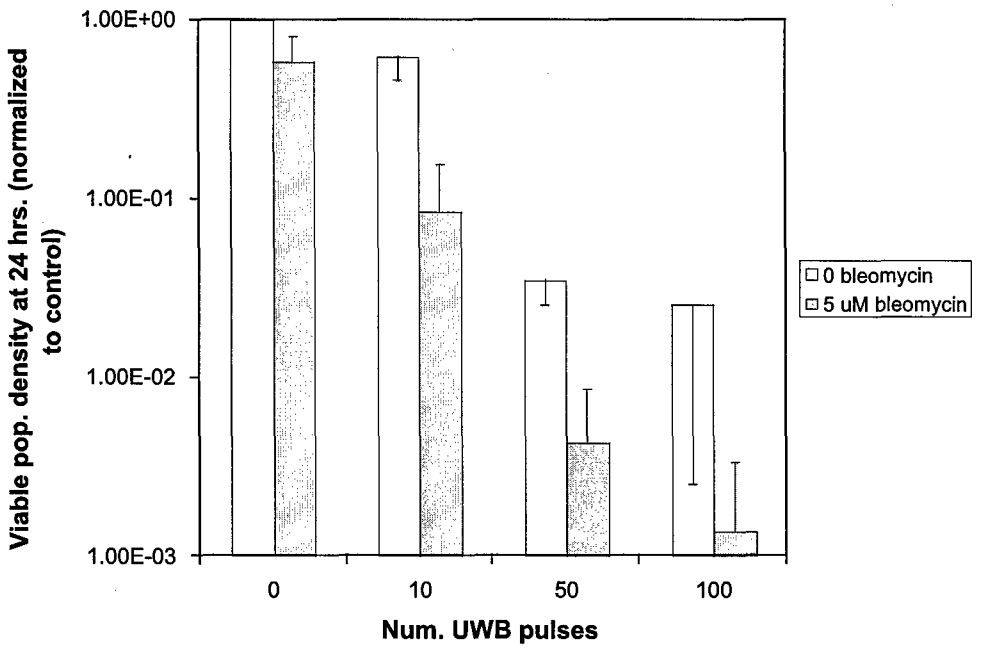

Figure 3.7. Viable cell number density (cells/ml), normalized to control, 24 hours after exposure to bleomycin and UWB pulses (95 kV/cm).

Clonogenic Viability of Cells exposed to UWB and UWB Electrochemotherapy

Clonogenic assays were performed to compare the membrane integrity of cells at 24 hours following UWB-ECT exposures (as measured by trypan blue staining) to the ability of cells to proliferate after treatment. Jurkat cells exposed to trains of 95 kV/cm pulses with 5 μM bleomycin and without bleomycin were evaluated. Assays were prepared and incubated for 7 days at 37° C under 5% CO_2. After dilution and incubation for 3-7 days, samples were evaluated by light microscopy and the dilution levels showing cell proliferation were noted. Figure 3.8 shows the results, plotted in terms of the sample dilution factor required to exclude clonogenically viable cells from each assay culture. This value gave a direct measurement of the density of clonogenically viable cells in the treatment sample at 24 hours post-exposure.

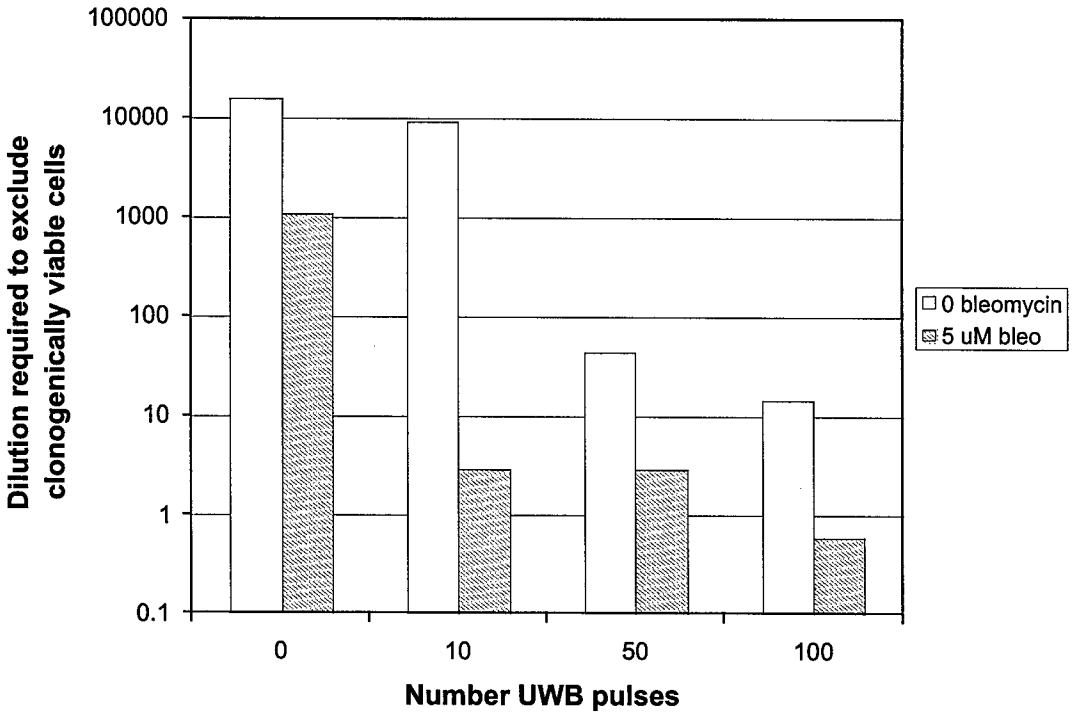

Figure 3.8. Clonogenic viability (at 24 hours post-exposure) of Jurkat cells exposed to 95 kV/cm UWB pulse trains and/or 5 μM bleomycin.

These data agreed with the trends shown in Figure 3.5, indicating that the proportion of cells that had recovered and maintained membrane integrity within 24 hours after exposure remained clonogenically viable. It was extremely unlikely that any long-term damage to components of intact cells (e.g. DNA or mitochondria) occurred that would enable a significant fraction of cells to exclude trypan blue at 24 hours but subsequently fail to divide.

Effect of Electric Field Strength on Bleomycin Delivery

It was noted from the data in Figure 3.8 that all UWB pulse treatments resulted in roughly the same level of clonogenic killing in the presence of bleomycin, a fact suggesting that 10 pulses was a sufficient treatment to deliver a saturated killing dose of bleomycin to the intracellular space. The experiment was repeated using a reduced electrode gap spacing (1 mm), resulting in pulse train average peak electric field strengths of 195 ± 5 kV/cm. The clonogenic assay results are presented in Figure 3.9.
For the increased electric field, a train of 5 pulses apparently resulted in the same saturation of bleomycin concentration within the cells. For 10 pulses at 95 kV/cm and 5 pulses at 195 kV/cm, the electric field stresses (expressed as the product of electric field and time) were roughly the same, lending further support to the conclusion that the UWB pulses electroporated the cell membrane to allow bleomycin uptake.

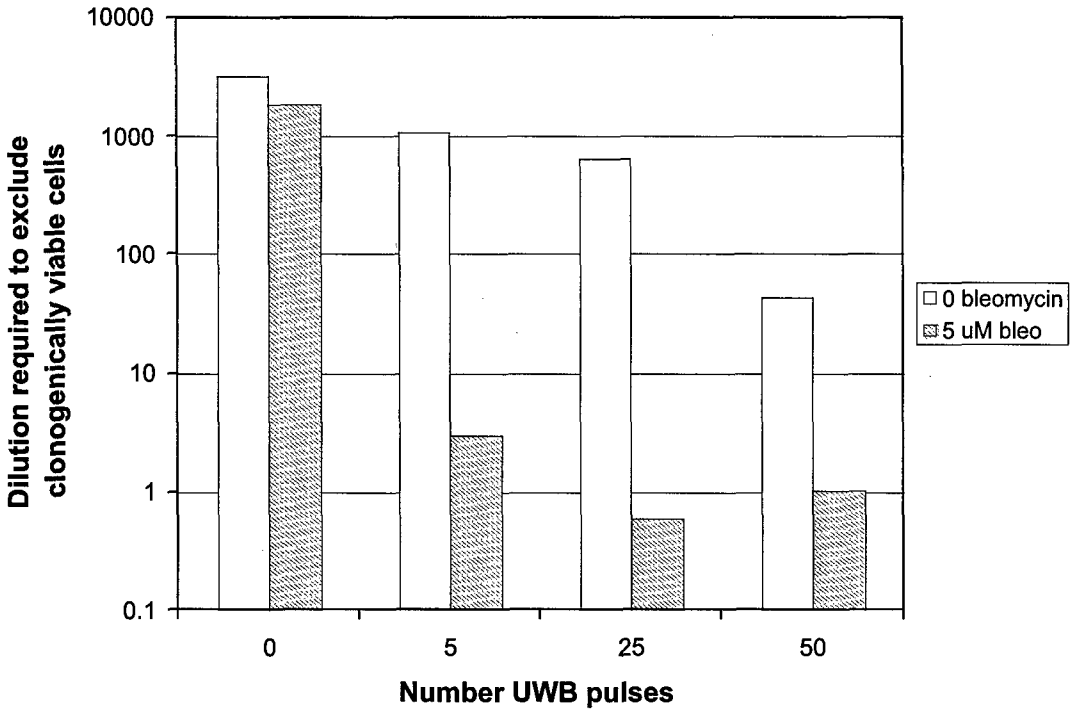

Figure 3.9. Clonogenic viability (at 24 hours post-exposure) of Jurkat cells exposed to 195 kV/cm UWB pulse trains and/or 5 μM bleomycin.

Since electroporation is a threshold phenomenon, experiments were performed with UWB pulses at a reduced electric field strength (50 kV/cm across a 4 mm gap) to test whether the 10 pulse treatment at 95 kV/cm was a necessary or merely sufficient condition to produce a maximum level of cell killing with bleomycin. The clonogenic assay results are shown in Figure 3.10. The reduced electric field (50 kV/cm) produced a saturation level of bleomycin killing for 10 pulses, indicating that the 95 kV/cm pulse train exceeded the electroporation threshold.

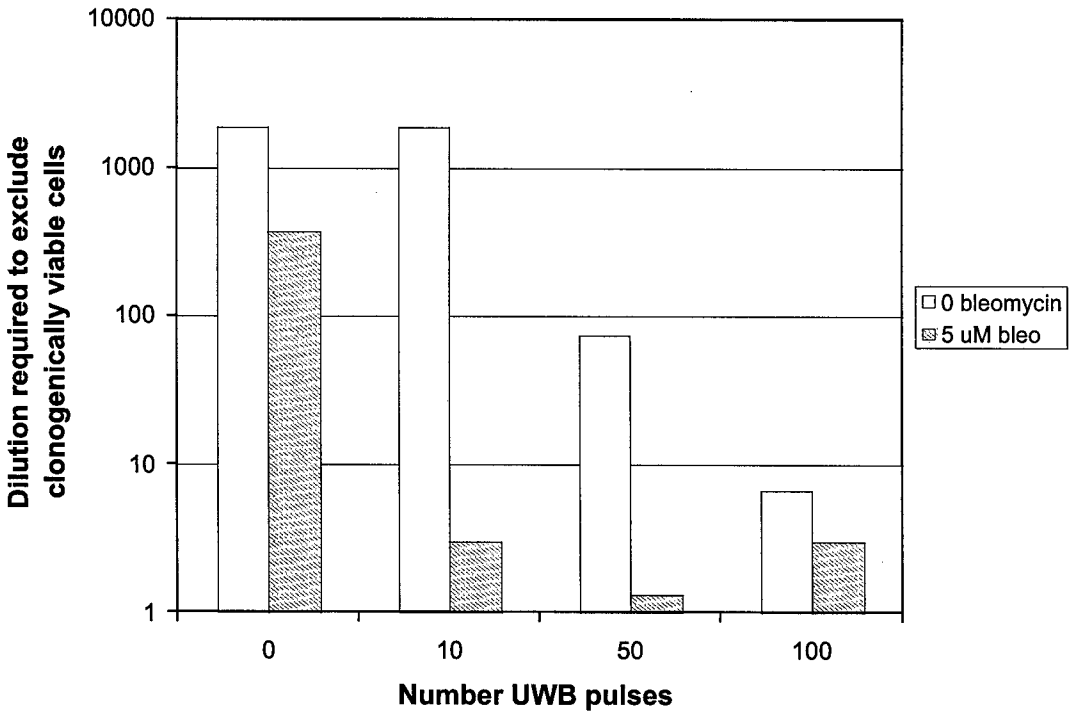

Figure 3.10. Clonogenic viability (at 24 hours post-exposure) of Jurkat cells exposed to 50 kV/cm UWB pulse trains and/or 5 μM bleomycin

Figure 3.11 directly compares the killing effects of trains of 10 UWB pulses at varied electric field strength on bleomycin-treated Jurkat cells. Viability was assessed by trypan blue staining at 24 hours, and the results were consistent with the clonogenic assay results observed over a range of field strengths (Figures 3.8 – 3.10). These data indicated that a train of 10 UWB pulses at 50 kV/cm caused sufficient electroporation to deliver a maximum lethal dose of bleomycin to cells from a 5 μM extracellular solution, and higher electric field strengths and longer pulse trains did not further enhance killing. Interestingly, these data also indicated that direct killing of Jurkat cells by trains of 10 UWB pulses (without bleomycin) was not significantly improved by increasing the average peak electric field strength from 50 to 195 kV/cm, even though increasing the number of pulses (pulse train length) did markedly increase the cell killing (Figure 3.3).

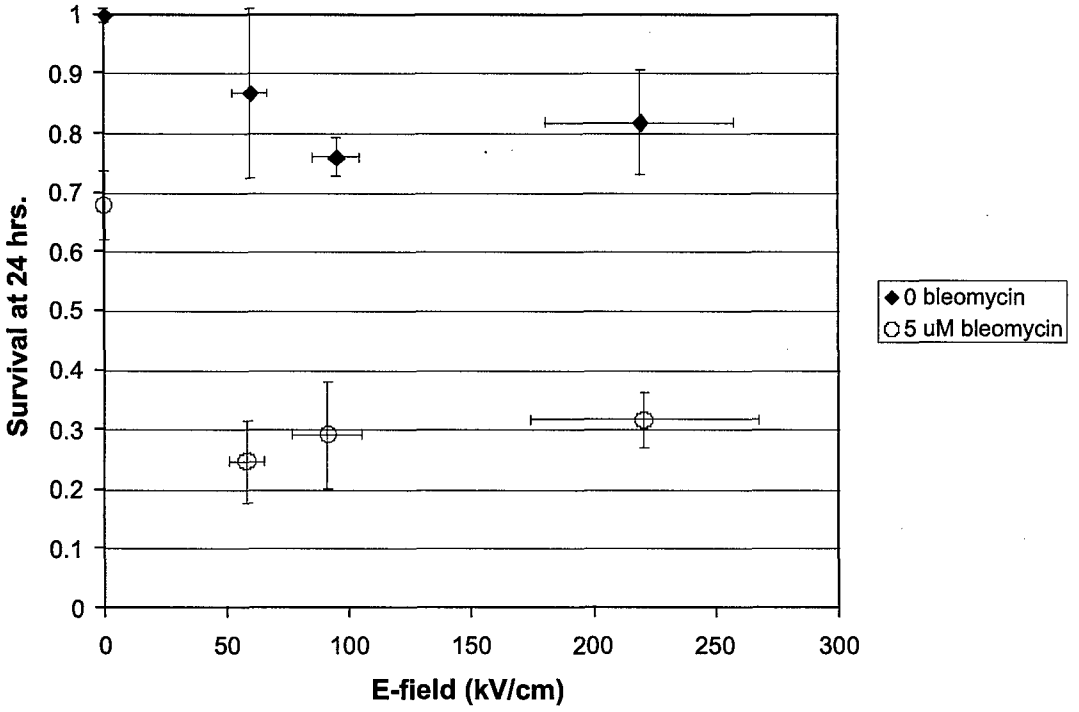

Figure 3.11. Viability (at 24 hours post-exposure) of Jurkat cells exposed to single trains of 10 UWB pulses with and without bleomycin for a range of peak electric fields (50-195 kV/cm).

Apoptosis Measurements in UWB and UWB Electrochemotherapy Exposures

Apoptosis, a form of programmed cell death, features several prominent biochemical responses that were measured to determine the mode of cell death for cells exposed to UWB pulses and UWB-ECT treatments. The activities of caspase-3 and caspase-7, enzymes involved in the deconstruction of cellular structures during apoptosis, were measured using a homogeneous luminescent assay (Caspase-Glo 3/7, Promega, Madison, WI). Phosphatidylserine (PS) inversion on the cell membrane was measured by fluorescence microscopy using an annexin V-FITC conjugate stain (Sigma, St. Louis, MO).

Caspase Activation in UWB and UWB Electrochemotherapy Exposures

Activation of caspases -3 and -7 in Jurkat cells exposed to trains of UWB pulses (95 kV/cm) and bleomycin solution was measured at 6 hours post-exposure. The measurement, presented in Figure 3.12, quantified the total activity of caspase-3 and caspase-7 in each cell sample as the brightness of a luciferase luminescence as measured by a photomultiplier. The luminescence value was reported in arbitrary units and was directly proportional to the mass of activated caspase enzyme in each sample.

A slight elevation of caspase activity was observed for cells exposed to trains of 10 pulses, regardless of the presence of bleomycin (Fig. 3.12). No significant difference was observed between sham controls and samples exposed to 50 or 100 pulses. The elevation observed for 10 pulses was small in magnitude (less than a factor of 2), suggesting that the primary mechanism of cell death in these samples was not an apoptotic pathway involving caspase activation.

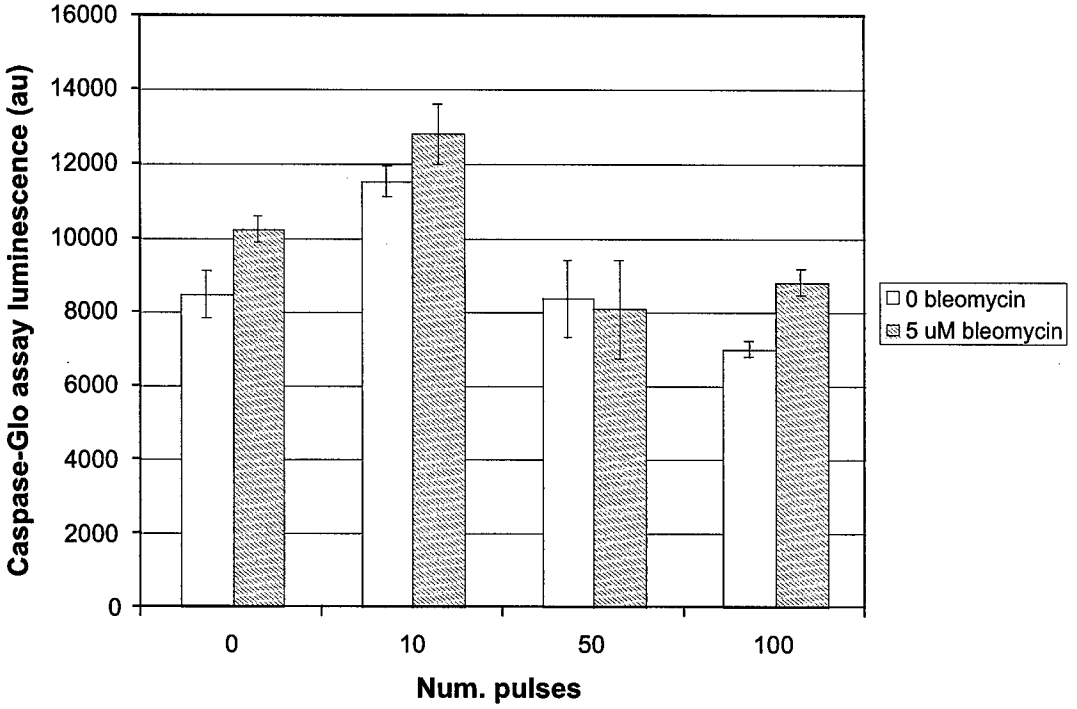

Figure 3.12. Caspase activity in Jurkat cells exposed to UWB pulses (95 kV/cm) with and without bleomycin at 6 hours post-exposure.

Phosphatidylserine Inversion in UWB and UWB Electrochemotherapy Exposures

Cells exposed to treatment with bleomycin, UWB pulses, or both were assayed for phosphatidylserine inversion as an apoptosis marker. Measurements were made at 1, 6, and 24 hour post-exposure time points. The two-stain system consisting of annexin V-FITC conjugate and propidium iodide (PI), was used. This system enabled the condition of cells to be determined from their staining properties as follows: viable, non-apoptotic cells exhibited no fluorescent staining and were visible only in the bright field; apoptotic cells were stained with fluorescent green labeling (annexin V-FITC); and dead cells were stained both green (annexin V-FITC) and red (PI). Images were captured using a monochrome digital camera and dichroic fluorescence filter sets, so each color was

imaged separately. A total of three images were collected for each field of view of each sample – a bright field, a dark field with red fluorescence detected, and a dark field with green fluorescence detected.
A two-color filter set (displaying green and red fluorescence simultaneously) was available for observation of samples. In Figure 3.13, a set of micrograph images has been reconstructed from monochromatic photographs to illustrate such a dual-fluorescence field of view. In analysis of these images, apoptosis would have been indicated by a large amount of green staining without accompanying red staining. In the images presented, no such increase in green staining was evident.

The complete quantitative data for phosphatidylserine inversion measurements are depicted in Figures 3.14, 3.15, and 3.16. These plots display the fraction of cells exhibiting PI and annexin V-FITC staining at 1, 6, and 24 hours post-exposure, respectively. In all cases except one, observed increases in green staining were accompanied by increases in red staining, indicating that the green fluorescence observed was due to dead, not apoptotic, cells. The single exception was for cells treated with combined UWB pulses and bleomycin at 6 hours post-exposure. A modest increase in annexin V-FITC staining was observed for these samples without an accompanying increase in PI staining, suggesting that a portion of the cells were apoptotic at 6 hours post-exposure.

Figure 3.15 contains an additional data series, the fraction of cells exhibiting apoptotic morphology. This determination was made on a cell-by-cell basis during examination of the bright field micrographs. Cells were noted as displaying apoptotic morphology if they were significantly smaller and more rounded than the typical cell in a control sample, or if they displayed other signs of apoptosis such as blebbing or formation of micronuclei. The fraction of cells expressing apoptotic changes in shape and size correlated closely to the fraction staining positive for PS inversion on the plasma membrane. Cells exposed to UWB pulses and bleomycin exhibited an increase in apoptotic morphology at 6 hours post-exposure.

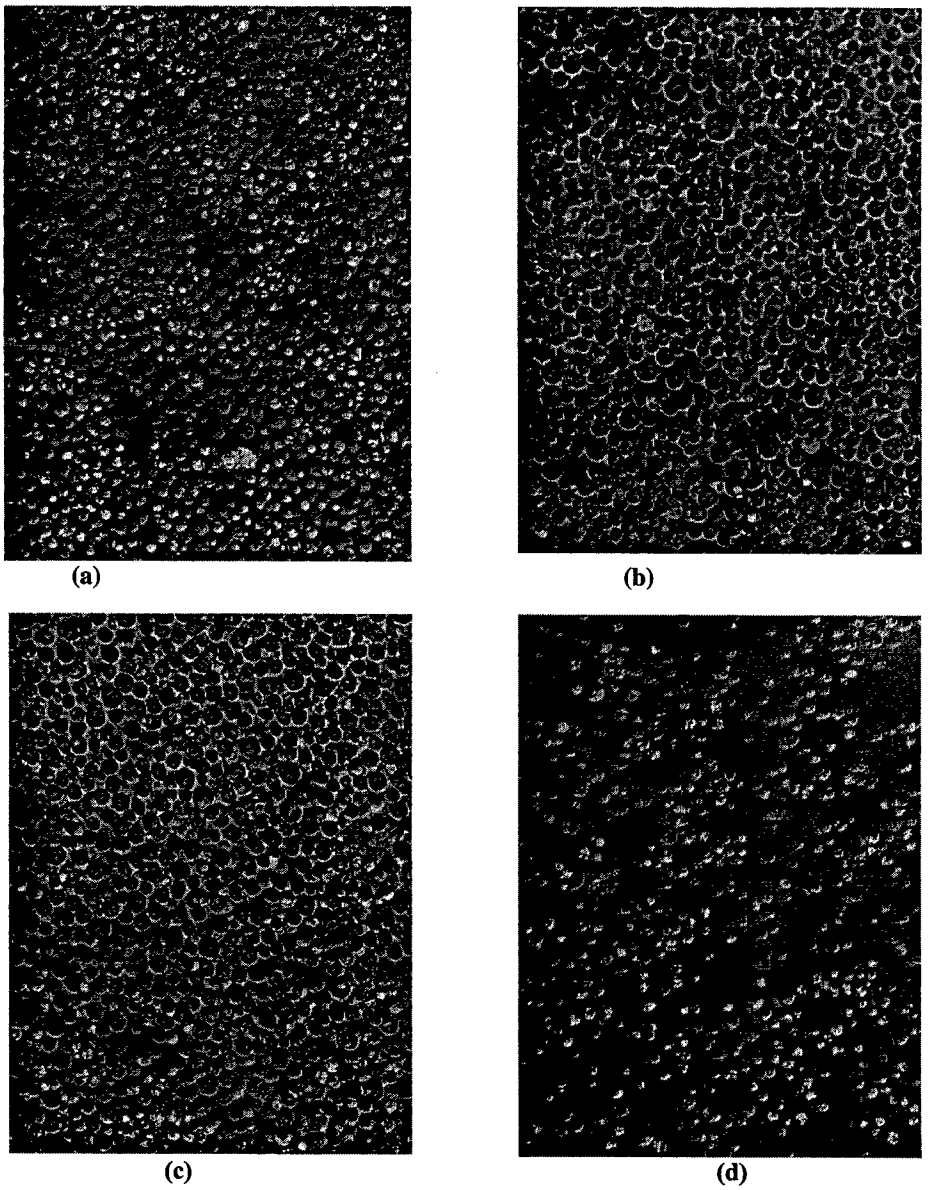

Figure 3.13. Composite fluorescence micrographs of Jurkat cells 24 hours after UWB pulse and 5 μM bleomycin treatment. Red staining indicates cell death. Green staining without red staining indicates apoptosis in progress.
(a) Untreated (sham) control cells.
(b) Cells subjected to 10 UWB pulses at 50 kV/cm.
(c) Cells subjected to 5 μM bleomycin.
(d) Cells subjected to 10 UWB pulses (50 kV/cm) and 5 μM bleomycin.

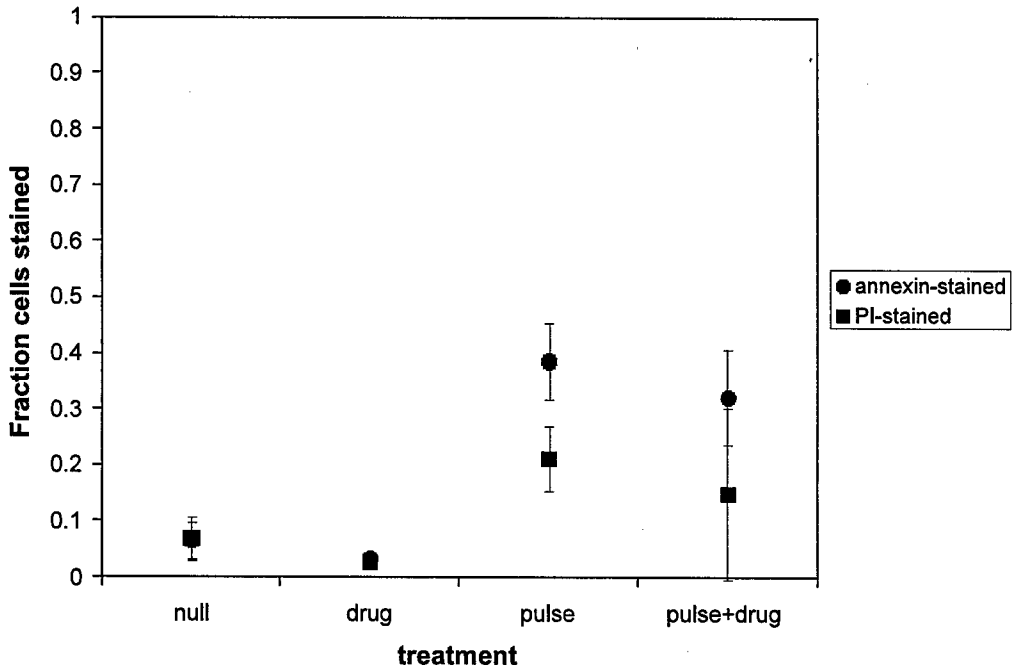

Figure 3.14. Jurkat cell death and PS inversion as measured by annexin V-FITC/PI staining at 1 hr. after exposure to UWB pulses and/or bleomycin.

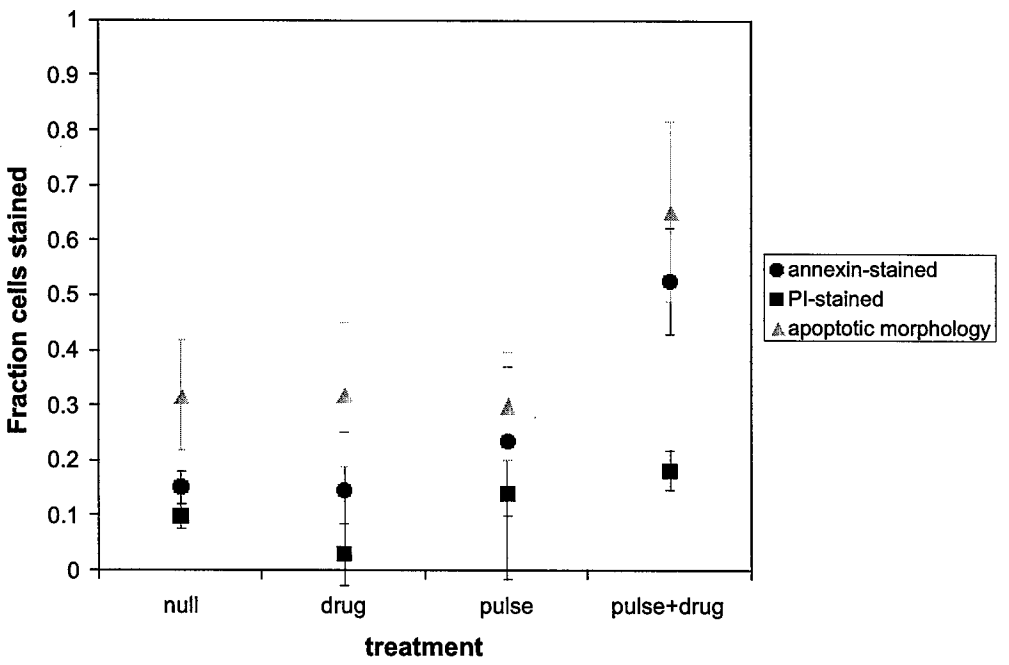

Figure 3.15. Jurkat cell death, PS inversion, and apoptotic morphology as measured by annexin V-FITC/PI staining at 6 hrs. after exposure to UWB pulses and/or bleomycin.

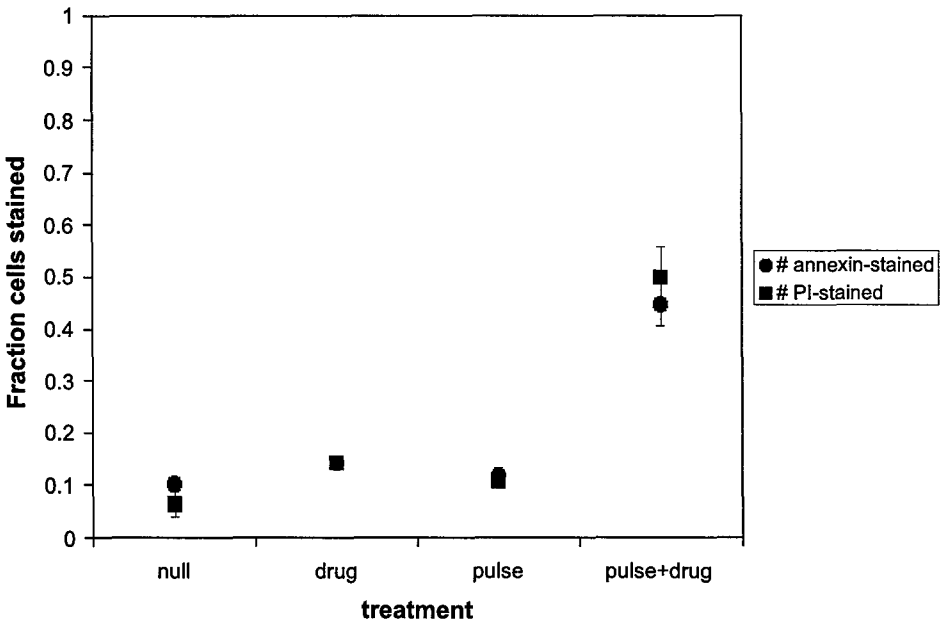

Figure 3.16. Jurkat cell death and PS inversion as measured by annexin V-FITC/PI staining at 24 hrs. after exposure to UWB pulses and/or bleomycin.

The striking feature revealed by the time course of the measurements presented in Figures 3.15 and 3.16 is that at 6 hours, approximately 50% of the cells exhibited PS inversion, and at 24 hours approximately 50% were dead. This indicates that for this combination of drug and UWB pulse treatments, the majority of cells that died did so slowly and expressed PS inversion on the plasma membrane. The weak activation of caspase at 6 hours suggests that caspase-dependent apoptosis was not the dominant mechanism of cell death. However, recent work has suggested that several other types of programmed cell death occur without activation of caspases. Such a mechanism may have been the endpoint of these cells; it seems logical that any programmed cell death would include a mechanism to label the cell for phagocytosis regardless of the involvement of caspase.

4. 0 Theory

Three areas were explored theoretically:

A. Thermal and nonthermal RF bioeffects in conventional electroporation experiments.

B. Thermal and nonthermal RF bioeffects using ultra-wideband source.

C. Electrode-less electroporation

A. The following estimates show that negligible heating occurred in the conventional electroporation. In our earlier experiments using the conventional electroporation generator, the maximum input power of 660 W for 2 ms was delivered into a sample volume of 100 μl; this gives a total energy of 1.3 J delivered to the sample. At room temperature, the maximum temperature increase (ΔT_{max}) in the sample during the pulse is governed by energy conservation,

$$\Delta T_{\max} = \frac{P_{inc} t_{on}}{\rho_m V_i C_P} = 3.1^o K \ , \qquad (1)$$

where P_{inc} = 660 W, t_{on} = 2 ms, V_i = 100 μl, and ρ_m = mass density = 1000kg/m^3, and C_P = specific heat = 4200 J/kg-K are taken to be water-like at 20° C.

B. The heating of cells by an ultra-wideband source requires consideration of the heating by the rf electric field and by the rf magnetic field. The investigators have recently provided a timely theory on this topic [W. Tang, H. Bosman, Y. Y. Lau, and R. M. Gilgenbach, J. Appl. Phys. **97**, 114915 (2005)] where the total energy absorbed by a particulate (which is to be used to model a cell), when it is exposed to a transient electromagnetic pulse may be calculated reliably.

The total energy, W_E, dissipated in the cell during this finite pulse through the rf electric field pulse is,

$$W_E = \int d\omega \alpha_E(\omega) \frac{1}{2} \omega \varepsilon_2 |E(\omega)|^2 V_a, \tag{2}$$

where α_E is the polarizability explicitly given in Tang et al. in terms of the electrical properties of the cell and $|E(\omega)|^2$ is Fourier spectrum of the electric field in the ultra-wideband pulse. Likewise, the total energy, W_M, absorbed by the cell through the rf magnetic field of the ultra-wideband pulse is given by

$$W_M = \int d\omega \alpha_H(\omega) \frac{1}{2} \omega \mu_2 |H(\omega)|^2 V_a, \tag{3}$$

where α_M is the polarizability for the rf magnetic field and $|H(\omega)|^2$ is the Fourier spectrum of the rf magnetic field in the ultra-wideband pulse.

Initial estimates show that the temperature rise due to the ultra-wideband pulse used in the experiments are negligible. Further investigation using Allen Garner's recent data

collected at ODU is underway, and the results will be presented in APS-DPP in Denver, CO in October, 2005.

C. At one point, it was thought that using an annular tube made of dielectric would create an electrode-less electroporation experiment if the cells under treatment are placed in the interior region of this dielectric tube, while the pulse is applied externally. It was also thought that this experiment might demonstrate action only through the displacement current, instead of the conduction current. A theoretical analysis of various electric field polarizations and geometries show that this is not the case. The main reason is that the conduction current is still dominant for electrical conductivity of order $1/(\Omega m)$, a typical average value for cellular medium. Another reason is that the wall of the dielectric tube accounts for most of the voltage drop.

5.0 Student, Faculty, and Staff Involvement in This research

Faculty:
Prof. R.M. Gilgenbach
Prof. Y.Y Lau
Prof. Michael D. Uhler

Staff
Linda Gates (Health Sciences Research Associate II)

Graduate Students:
1) David Jordan (Ph.D. Candidate)
2) Allen Garner (Ph.D. Candidate)
3) Ho Yin Chan (PhD Pre-candidate)

Undergraduate Students
1) Elizabeth Coon
2) Kris Ball
3) Hong Chong

6.0 Relevant Publications and Conference Papers by UM Faculty and Students (includes collaborations with Old Dominion University)

Refereed Journals

1) D. Jordan, R.M. Gilgenbach, M.D. Uhler, L.H. Gates, and Y. Y. Lau, "Effect of Pulsed, High-Power Radiofrequency Radiation on Electroporation of Mammalian Cells", IEEE Transactions on Plasma Science, Special Issue on Bioeffects, Vol 32, p 1573, October, 2004

2) Allen L. Garner, Y. Y. Lau, David W. Jordan, Michael D. Uhler, and Ronald M. Gilgenbach, "Implications of a Simple Mathematical Model to Cancer Cell Population Dynamics," *Cell Proliferation*, submitted, July 2005.

3) Allen L. Garner, Y. Y. Lau, Michael D. Uhler, David W. Jordan, and Ronald M. Gilgenbach, "Incorporating Spatial Dependence Into a Multicellular Tumor Spheroid Growth Model," *Journal of Applied Physics*, submitted, July 2005.

4) George Chen, Nianyong Chen, Allen L. Garner, Juergen Kolb, R. James Swanson, Stephen J. Beebe, Ravindra P. Joshi, and Karl H. Schoenbach, "Conductivity in Jurkat Cell Suspension after Ultrashort Electric Pulsing," *Biophysical Journal*, submitted Feb 2005.

Conference Papers:

1) D. W. Jordan, A. L. Garner, R. M. Gilgenbach, M. D. Uhler, L. Gates, Y. Y. Lau. "Frequency Dependence of Electroporation of Mammalian Cells by Pulsed High Power Radiofrequency Radiation," 2004 IEEE International Conference on Plasma Science, p. 194 (2004).

2) D.W. Jordan R.M. Gilgenbach, M.D. Uhler, A. Garner, Y.Y. Lau, "Ultrawideband Irradiation Effects on Chemotherapy of Jurkat Cells", ElectroMed 2005, May 16-18, 2005, Portland, Oregon

3) D.W. Jordan, R.M. Gilgenbach, M.D. Uhler, A.L. Garner, L. Gates, Y.Y. Lau, "Membrane Effects of Pulsed High Power Radiofrequency Radiation in Mammalian Cells," Bioelectromagnetics Society Annual Meeting, June 2004, Washington, DC.

4) G. Chen, N. Chen, A.L. Garner, J. Kolb, R.J. Swanson, S. Beebe, R.P. Joshi, K.H. Schoenbach, "Conductivity in Jurkat Cell Suspension after Ultrashort Electric Pulsing," Proceedings of the 3rd International Workshop on Biological Effect of EMFs, Kos, Greece, Vol. 1, pp. 56-65 (2004).

5) Allen L. Garner, David W. Jordan, Wilkin Tang, Y. Y. Lau, Ronald M. Gilgenbach, and Michael D. Uhler, "Ohmic Heating of Electrically Pulsed Biological Cells in Suspension," American Physical Society Division of Plasma Physics, October 2005, submitted.

6) A.L. Garner, D.W. Jordan, Y.Y. Lau, M.D. Uhler, R.M. Gilgenbach, "Analysis and Application of a Cell Population Model for Electrically Pulsed Cells," Electromed 2005, May 2005, Portland.

7) A.L. Garner, J. Yang, N. Chen, J. Kolb, K.C. Loftin, R.J. Swanson, S. Beebe, R.P. Joshi, K.H. Schoenbach, "Altering Dielectric Properties of Human Cancer Cells by Varying Electrical Pulse Duration," 2004 IEEE International Conference on Plasma Science, p. 195 (2004).

8) A.L. Garner, J. Yang, N. Chen, J. Kolb, K.C. Loftin, R.J. Swanson, S. Beebe, R.P. Joshi, K.H. Schoenbach, "Electrical Pulse-Induced Changes in HL-60 Dielectric Properties," Bioelectromagnetics Society Annual Meeting, June 2004, Washington, DC.

9) *A. L. Garner*, G. Chen, N. Chen, V. Sridhara, J.F. Kolb, R.J. Swanson, R.P. Joshi, K.H. Schoenbach, "Changes in the Dielectric Properties of Jurkat and HL-60 Cells after Electrical Pulses," Electromed 2005, May 2005, Portland, Oregon.